

# Triple $Z^0$ -boson production in large extra dimensions model at ILC

Jiang Ruo-Cheng, Li Xiao-Zhou, Ma Wen-Gan, Guo Lei, and Zhang Ren-You  
Department of Modern Physics, University of Science and Technology  
of China (USTC), Hefei, Anhui 230026, P.R.China

## Abstract

We investigate the effects induced by the interactions of the Kaluza-Klein (KK) graviton with the standard model (SM) particles on the triple  $Z^0$ -boson production process at the ILC in the framework of the large extra dimension (LED) model. We present the dependence of the integrated cross sections on the electron-positron colliding energy  $\sqrt{s}$ , and various kinematic distributions of final  $Z^0$  bosons and their subsequential decay products in both the SM and the LED model. We also provide the relationship between the integrated cross section and the fundamental scale  $M_S$  by taking the number of the extra dimensions ( $d$ ) as 3, 4, 5, and 6, respectively. The numerical results show that the LED effect can induce a observable relative discrepancy for the integrated cross section ( $\delta_{LED}$ ), which can reach the value of 13.11% (9.27%) when  $M_S = 3.5$  (3.8)  $TeV$  and the colliding energy  $\sqrt{s} = 1$   $TeV$ . We find the relative discrepancy of LED effect can even reach few dozen percent in the high transverse momentum area or the central rapidity region of the final  $Z^0$ -bosons and muons.

**PACS:** 11.10.Kk, 13.66.Fg, 14.70.Hp

## I. Introduction

The large extra dimensions (LED) model, proposed by Arkani-Hamed, Dimopoulos and Dvali (ADD) [1], is an attractive extension of the standard model (SM) because of its possible testable consequences. In the LED model only graviton can propagate in a  $D = 4 + d$  dimensional space with  $d$  being the dimension number of extra space, while the SM particles exist in the usual  $(3 + 1)$ -dimensional space. The picture of a massless graviton propagating in  $D$ -dimensions is equal to the scene where numerous massive Kaluza-Klein (KK) gravitons propagate in  $(3 + 1)$ -dimensions. So we can expect that even though the gravitational interactions in the 4 space-time dimensions are suppressed by a factor of  $1/M_P$ , they can be compensated by these numerous KK states. Therefore, in either the case of real graviton emission or the case of virtual graviton exchange, it is shown that the Plank mass  $M_P$  cancels out of the cross section after summing over the KK states, and we can obtain an interaction strength comparable to the electroweak strength [2, 3]. Up to now, many works on the LED phenomenology at colliders have been done, including vector boson pair productions and association productions of vector boson with graviton [4, 5, 6].

The precision measurements of the trilinear gauge boson couplings (TGCs) are helpful for verification of non-Abelian gauge structure, and the investigation of the quartic gauge boson couplings (QGCs) can either confirm the symmetry breaking mechanism or present a direct test on the new physics beyond the SM. The vector boson pair production processes were extensively studied in the SM for probing the TGCs [7, 8, 9, 10, 11]. The direct study of QGCs requires the investigation of the processes involving at least three external gauge bosons. Recently, the triple  $Z^0$ -boson production in the LED model at the LHC was studied in Ref.[12].

The International Linear Collider (ILC) is proposed with the colliding energy  $\sqrt{s} = 200 \sim 500 \text{ GeV}$  which would be upgraded to  $\sqrt{s} = 1 \text{ TeV}$ , and the integrated luminosity is required to be  $1000 \text{ fb}^{-1}$  in the first phase of operation [11]. The triple gauge boson productions at the ILC are important processes in probing the TGCs and QGCs of electroweak theory, which are related to electroweak symmetry breaking mechanism. If their observables coincide with the LED predictions on the triple gauge boson production processes, it means the coupling of graviton to

gauge bosons in the LED model would be the causation. Therefore, the understanding of the LED phenomenology in triple gauge boson production processes at the ILC is necessary.

In this paper we study the LED effects on the process  $e^+e^- \rightarrow Z^0 Z^0 Z^0$  at the ILC. The paper is organized as follows: In section II we present the calculation descriptions for the process with a brief review of the related LED theory. The numerical results and discussions are given in section III. In the last section a short summary is given.

## II. Analytic calculations

In the LED model, the extra dimensions on a torus are compactified to a radius  $R/2\pi$ . The relationship between the usual Planck scale  $M_P$  to the fundamental scale  $M_S$  is

$$M_P^2 = \frac{2(4\pi)^{-d/2}}{\Gamma(d/2)} M_S^{2+d} R^d \quad (2.1)$$

where  $M_P = 1/\sqrt{G_N} \sim 1.22 \times 10^{19} \text{ GeV}$  and  $G_N$  is Newton's constant. In our work we use the de Donder gauge for the pure KK-graviton part and the Feynman gauge ( $\xi = 1$ ) for the SM part. The Feynman rules for the relevant vertices including KK graviton used in our calculations are given below [13], where we assume that all the momenta flow to the vertices, except that the fermionic momenta are set to be along the fermion flow directions.

- $G_{\text{KK}}^{\mu\nu}(k_3) - \bar{\psi}(k_1) - \psi(k_2)$  vertex :

$$-i\frac{\kappa}{8} [\gamma^\mu(k_1 + k_2)^\nu + \gamma^\nu(k_1 + k_2)^\mu - 2\eta^{\mu\nu}(k_1 + k_2 - 2m_\psi)], \quad (2.2)$$

- $G_{\text{KK}}^{\mu\nu}(k_3) - Z^\rho(k_1) - Z^\sigma(k_2)$  vertex :

$$i\kappa \left[ B^{\mu\nu\rho\sigma} m_Z^2 + (C^{\mu\nu\rho\sigma\tau\beta} - C^{\mu\nu\rho\beta\sigma\tau}) k_{1\tau} k_{2\beta} + \frac{1}{\xi} E^{\mu\nu\rho\sigma}(k_1, k_2) \right], \quad (2.3)$$

- $G_{\text{KK}}^{\mu\nu}(k_4) - \bar{\psi}(k_1) - \psi(k_2) - Z^\rho(k_3)$  vertex :

$$ie\frac{\kappa}{4} (\gamma^\mu \eta^{\nu\rho} + \gamma^\nu \eta^{\mu\rho} - 2\gamma^\rho \eta^{\mu\nu}) (v_f - a_f \gamma^5), \quad (2.4)$$

where  $G_{\text{KK}}^{\mu\nu}$ ,  $\psi$  and  $Z^\mu$  represent the fields of graviton, lepton, and  $Z^0$ -boson, respectively,  $e = g \sin \theta_W$  is the positron electric charge,  $\xi$  is the  $SU(2)$  gauge fixing parameter,  $v_f$ ,  $a_f$  are

the vector and axial-vector couplings which are the same as those defined in the SM, and  $\kappa = \sqrt{16\pi G_N} = \sqrt{2}/\overline{M}_P$  where the reduced Planck scale  $\overline{M}_P = M_P/\sqrt{8\pi}$ . The explicit expressions for the tensor coefficients are given as

$$\begin{aligned}
B^{\mu\nu\alpha\beta} &= \frac{1}{2}(\eta^{\mu\nu}\eta^{\alpha\beta} - \eta^{\mu\alpha}\eta^{\nu\beta} - \eta^{\mu\beta}\eta^{\nu\alpha}), \\
C^{\rho\sigma\mu\nu\alpha\beta} &= \frac{1}{2}[\eta^{\rho\sigma}\eta^{\mu\nu}\eta^{\alpha\beta} - (\eta^{\rho\mu}\eta^{\sigma\nu}\eta^{\alpha\beta} + \eta^{\rho\nu}\eta^{\sigma\mu}\eta^{\alpha\beta} + \eta^{\rho\alpha}\eta^{\sigma\beta}\eta^{\mu\nu} + \eta^{\rho\beta}\eta^{\sigma\alpha}\eta^{\mu\nu})], \\
E^{\mu\nu\rho\sigma}(k_1, k_2) &= \eta^{\mu\nu}(k_1^\rho k_1^\sigma + k_2^\rho k_2^\sigma + k_1^\rho k_2^\sigma) - [\eta^{\nu\sigma} k_1^\mu k_1^\rho + \eta^{\nu\rho} k_2^\mu k_2^\sigma + (\mu \leftrightarrow \nu)].
\end{aligned} \tag{2.5}$$

After summation over KK states the spin-2 KK graviton propagator can be expressed as [?]

$$\tilde{G}_{\text{KK}}^{\mu\nu\alpha\beta} = \frac{1}{2}D(s) \left[ \eta^{\mu\alpha}\eta^{\nu\beta} + \eta^{\mu\beta}\eta^{\nu\alpha} - \frac{2}{d+2}\eta^{\mu\nu}\eta^{\alpha\beta} \right], \tag{2.6}$$

where

$$D(s) = \frac{16\pi}{\kappa^2} \frac{s^{d/2-1}}{M_S^{d+2}} \left[ \pi + 2iI(\Lambda/\sqrt{s}) \right], \tag{2.7}$$

and

$$I(\Lambda/\sqrt{s}) = P \int_0^{\Lambda/\sqrt{s}} dy \frac{y^{d-1}}{1-y^2}. \tag{2.8}$$

The integral  $I(\Lambda/\sqrt{s})$  should be understood that a point  $y = 1$  has been removed from the integration path, and we set the ultraviolet cutoff  $\Lambda$  to be the fundamental scale  $M_S$  routinely.

We denote the process of the triple  $Z^0$ -boson production at the ILC as

$$e^+(p_1) + e^-(p_2) \rightarrow Z^0(p_3) + Z^0(p_4) + Z^0(p_5). \tag{2.9}$$

The SM-like diagrams for the above process are depicted in Fig.1(a). In the LED model, the KK graviton can couple to  $Z^0$ -pair and fermion-pair. We present the four additional pure LED Feynman diagrams in Fig.1(b).

In our calculations the developed FeynArts3.4 package [14] is adopted to generate all the lowest order Feynman diagrams and convert them to the corresponding amplitudes. Subsequently, the amplitude calculations are mainly implemented by applying modified FormCalc5.4 programs [15].

### III. Numerical results and discussions

In our numerical calculations, we use the following set of input parameters [17]:

$$m_W = 80.385 \text{ GeV}, m_Z = 91.1876 \text{ GeV}, \alpha_{ew}(0) = 1/137.036,$$

$$\sin^2 \theta_W = 1 - m_W^2/m_Z^2 = 0.222897, m_e = 0.510998928 \text{ MeV}.$$

We know that the ATLAS and CMS experiments found several SM Higgs-like events at the location of  $M_H \sim 125 \text{ GeV}$  [18]. Recently, ATLAS reported the searching for extra dimensions by using diphoton events in  $\sqrt{s} = 7 \text{ TeV}$   $pp$  collisions [19]. The results provided 95% C.L. lower limits on the fundamental Planck scale  $M_S$  between  $2.27 \text{ TeV}$  and  $3.53 \text{ TeV}$  depending on the number of extra dimensions  $d$  in the range of 7 to 3. The diphoton and dilepton results from CMS set limits on  $M_S$  in the range of  $2.5 - 3.8 \text{ TeV}$  as  $d$  varies from 7 to 2 at 95% C.L. [20]. In this work we take  $M_H = 125 \text{ GeV}$ , and set  $M_S = 3.5 \text{ TeV}$  (or  $M_S = 3.8 \text{ TeV}$ ) and  $d = 3$  as the representative ADD parameters in case otherwise stated.

In Refs.[10, 11] there exist the calculations for the SM one-loop electroweak corrections to the  $e^+e^- \rightarrow Z^0Z^0Z^0$  process. We make comparison of our LO numerical results with theirs, there we adopt the input parameters equal to those in Ref.[10] and use two different packages in order to check the correctness of our LO calculations. In Table 1 we present the results of the LO integral cross sections in the SM at the  $\sqrt{s} = 500 \text{ GeV}$  ILC obtained by using CompHEP-

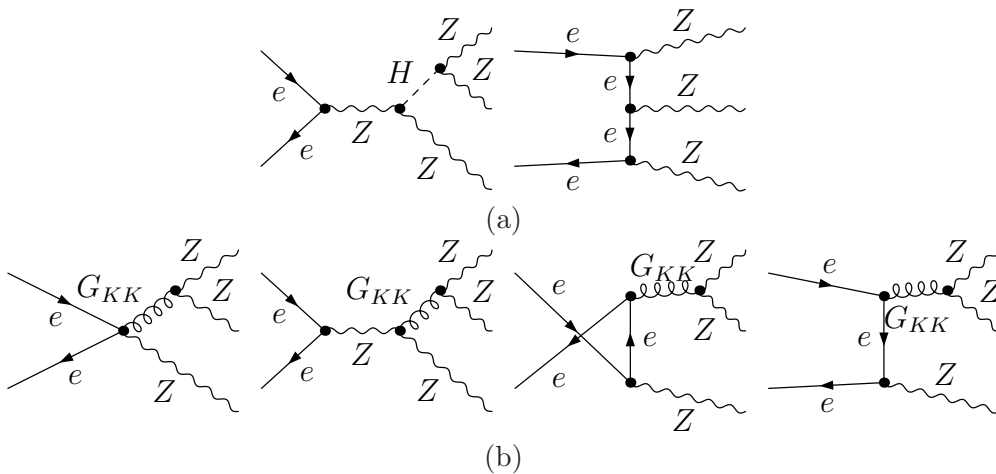


Figure 1: The Feynman diagrams for the process  $e^+e^- \rightarrow Z^0Z^0Z^0$  in the LED model. (a) The SM-like diagrams. (b) The additional diagrams with KK graviton exchange.

$M_H$ ( $GeV$ )	$\sigma_{SM}$ ( $fb$ ) at LO		
	CompHEP	FeynArts	Ref.[10]
115	1.0053(3)	1.0055(1)	1.0055(2)
120	1.0136(3)	1.0138(1)	1.0138(2)
150	1.0974(3)	1.0974(1)	1.0975(2)
170	1.2563(4)	1.2564(1)	1.2564(2)

Table 1: The numerical results of the LO integral cross sections for the process  $e^+e^- \rightarrow Z^0Z^0Z^0$  in the SM at the  $\sqrt{s} = 500 GeV$  ILC by using CompHEP-4.5.1 and FeynArts3.4/FormCalc5.3 packages, and the LO  $\sigma_{SM}$  by using FeynArts3.3/FormCalc5.3 package provided in Table 1 of Ref.[10].

4.5.1 [16] and FeynArts3.4/FormCalc5.4 packages separately, and the LO  $\sigma_{SM}$  results by using FeynArts3.3/FormCalc5.3 package presented in Table 1 of Ref.[10]. We can see that all the corresponding cross sections are in good agreement within the calculation errors.

In the upper plot of Fig.2 we present the numerical results of the LO integrated cross sections for the process  $e^+e^- \rightarrow Z^0Z^0Z^0$  as functions of the colliding energy  $\sqrt{s}$  in both the SM and the LED model. The curves reveal that the integrated cross section increases rapidly when  $\sqrt{s} < 500 GeV$  and decreases smoothly when  $\sqrt{s} > 600 GeV$ . Obviously, we can find that the curve for the LED model decreases more slowly than that for the SM in the region of  $\sqrt{s} > 600 GeV$ . We define the relative discrepancy as  $\delta_{LED} \equiv \frac{\sigma_{LED} - \sigma_{SM}}{\sigma_{SM}}$  to describe the LED effect on the integral cross section for the process  $e^+e^- \rightarrow Z^0Z^0Z^0$ , and plot its distribution versus  $\sqrt{s}$  in the nether plot of Fig.2. We can read out from Fig.2 that the LED relative discrepancies at the positions of  $\sqrt{s} = 500 GeV$ ,  $800 TeV$ , and  $1 TeV$  are 1.15% (0.83%), 5.69% (4.07%), and 13.11% (9.27%) for  $M_S = 3.5$  (3.8)  $TeV$ , separately. The LED relative discrepancy  $\delta_{LED}$  goes up as the increment of the colliding energy  $\sqrt{s}$ , and the enhancement of the cross section  $\sigma_{LED} - \sigma_{SM}$  becomes larger and larger when the colliding energy  $\sqrt{s}$  goes beyond  $600 GeV$ .

In analyzing the  $e^+e^- \rightarrow Z^0Z^0Z^0$  event, we classify the final three  $Z^0$  bosons as the leading  $Z^0$ -boson, the next-to-leading  $Z^0$ -boson and the next-to-next-to-leading  $Z^0$ -boson according to their transverse momenta, labeled as  $Z_1$ ,  $Z_2$  and  $Z_3$ , respectively. The criterion for final  $Z^0$ -boson clarification is based on the conditions of  $p_T^{Z_1} > p_T^{Z_2} > p_T^{Z_3}$ . In Fig.3 we present the distributions of the transverse momenta of  $Z_{1,2,3}$ -bosons in the SM and the LED model, and the corresponding

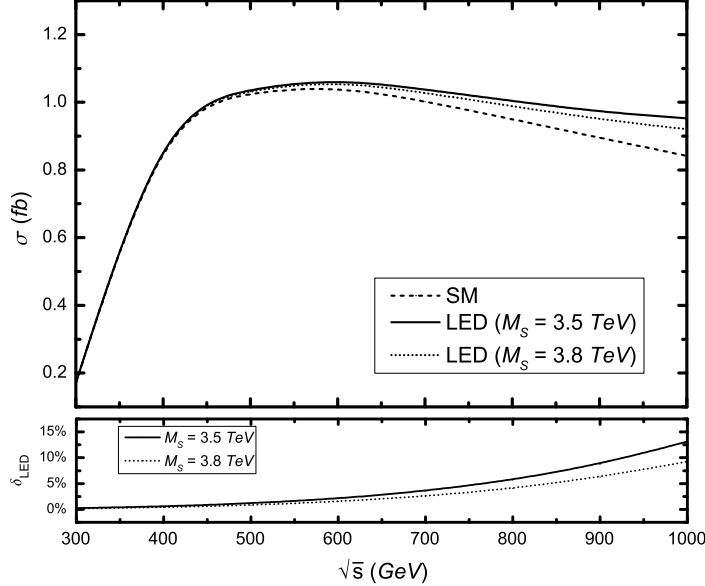


Figure 2: The integrated cross sections for the process  $e^+e^- \rightarrow Z^0Z^0Z^0$  in both the SM and the LED model, and the relative discrepancy due to the LED effect ( $\delta_{LED} \equiv \frac{\sigma_{LED} - \sigma_{SM}}{\sigma_{SM}}$ ), as functions of the colliding energy  $\sqrt{s}$  by taking  $M_S = 3.5$  TeV, 3.8 TeV and  $d = 3$ .

relative discrepancies,  $\frac{d\sigma_{SM}}{dp_T^{Z_{1,2,3}}}$ ,  $\frac{d\sigma_{LED}}{dp_T^{Z_{1,2,3}}}$ ,  $\delta_{LED}(p_T^{Z_{1,2,3}})$  in the conditions of  $M_S = 3.5$  TeV, 3.8 TeV,  $\sqrt{s} = 800$  GeV, 1 TeV, separately. The curves in Fig.3 show that the LED effect enhances the differential cross section, particularly in the relative high transverse momentum region. We can see that in the conditions of  $\sqrt{s} = 800$  GeV and  $M_S = 3.5$  (3.8) TeV, the relative discrepancies  $\delta_{LED}(p_T^{Z_{1,2,3}})$  can reach the maximal values of 11.08% (8.27%), 13.54% (9.92%) and 8.72% (6.17%) separately, while in the conditions of  $\sqrt{s} = 1$  TeV and  $M_S = 3.5$  (3.8) TeV, the maximum values of  $\delta_{LED}(p_T^{Z_{1,2,3}})$  are increased to be 29.75% (21.39%), 41.14% (27.96%), and 19.94% (14.35%), respectively. The curves for the differential cross sections of  $p_T^{Z_1}$  in Figs.3(a,b) demonstrate the maxima values of  $\delta_{LED}(p_T^{Z_1})$  are located at the vicinities of  $p_T^{Z_1} = 310$  GeV and  $p_T^{Z_1} = 410$  GeV at the  $\sqrt{s} = 800$  GeV and 1 TeV ILC respectively, while Fig.7 in Ref.[12] shows the relative discrepancy increases monotonously with the increment of  $p_T^{Z_1}$  at the LHC.

The rapidity distributions of final  $Z$ -bosons in the SM and the LED model,  $d\sigma_{SM,LED}/dy^{Z_{1,2,3}}$ , and the corresponding LED relative discrepancies,  $\delta_{LED}(y^{Z_{1,2,3}})$ , with  $M_S = 3.5$  TeV, 3.8 TeV and  $\sqrt{s} = 800$  GeV, 1 TeV are shown in Figs.4(a-f), respectively. The line-shapes of  $y^{Z_1}$  and  $y^{Z_2}$  distributions are similar, while the  $y^{Z_3}$  distribution seems to be particular. All the curves

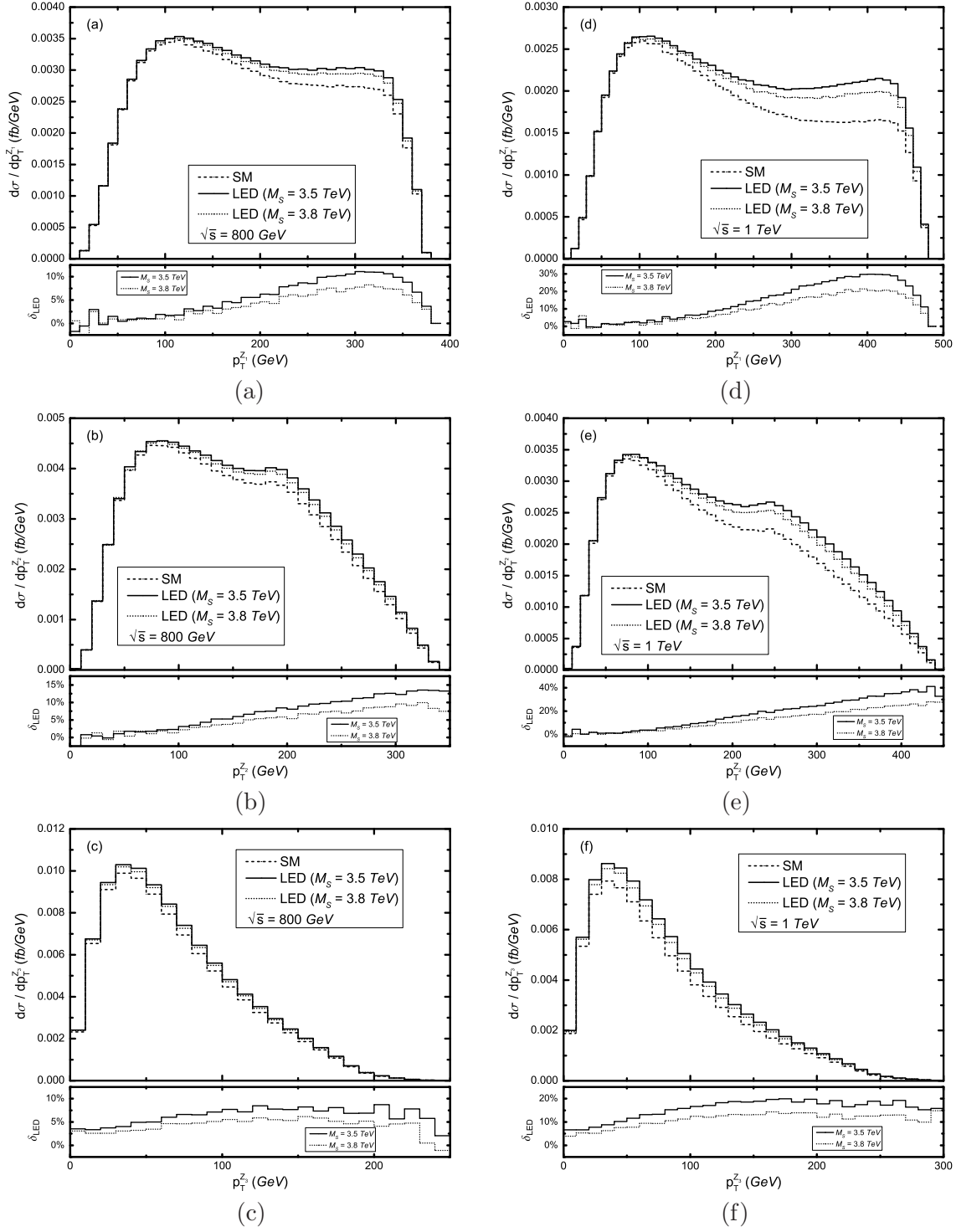


Figure 3: The distributions of the transverse momenta of  $Z^0$ -bosons in the SM and the LED model, and the corresponding relative discrepancies, defined as  $\delta_{LED}(p_T^Z) \equiv \left( \frac{d\sigma_{LED}}{dp_T^Z} - \frac{d\sigma_{SM}}{dp_T^Z} \right) / \frac{d\sigma_{SM}}{dp_T^Z}$ , with  $M_S = 3.5, 3.8$  TeV and  $d = 3$ . Plots (a), (b) and (c) are for the  $p_T^{Z_1}$ ,  $p_T^{Z_2}$  and  $p_T^{Z_3}$  distributions at the  $\sqrt{s} = 800$  GeV ILC, while (d), (e) and (f) are for the  $p_T^{Z_{1,2,3}}$  distributions at the  $\sqrt{s} = 1$  TeV ILC, respectively.



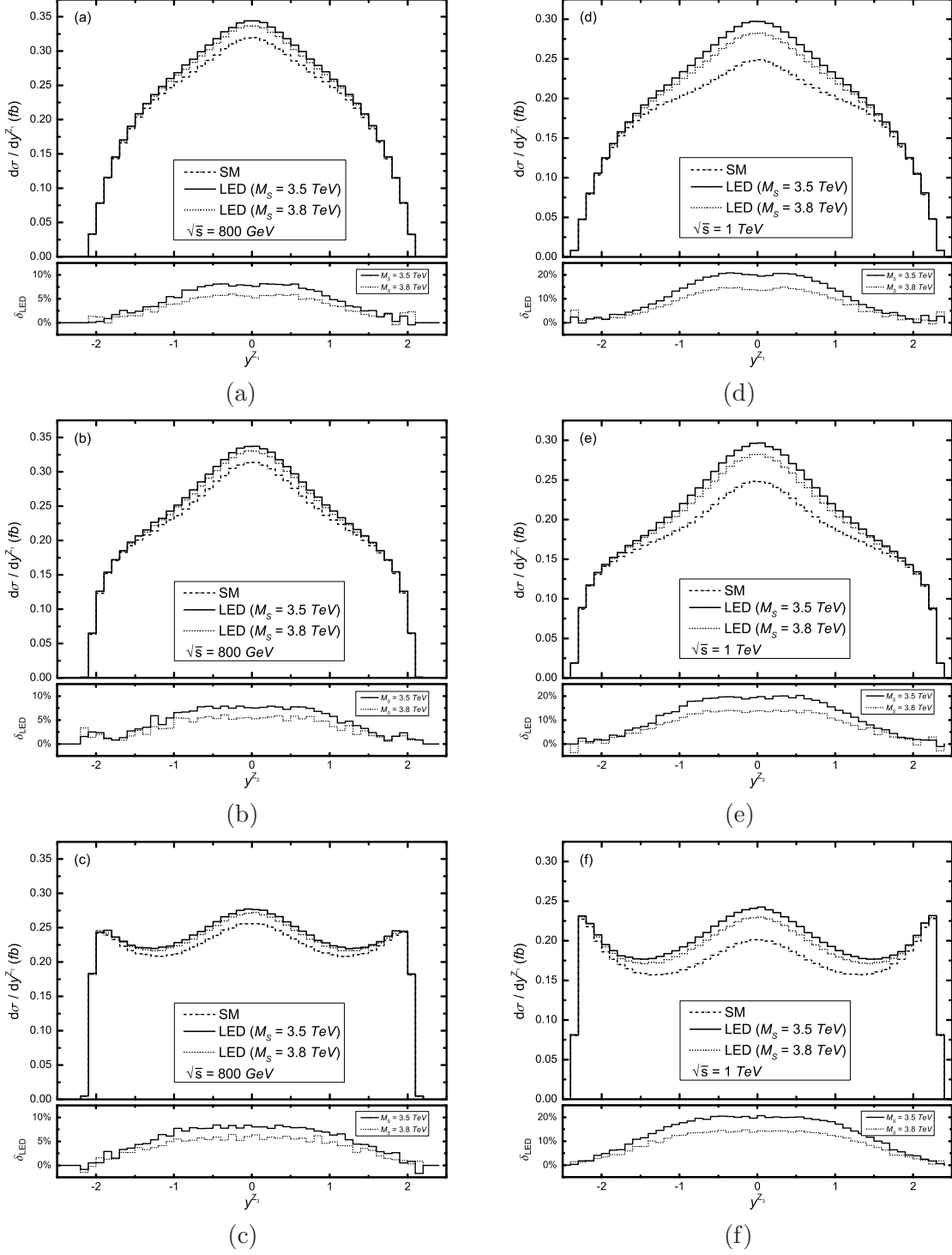


Figure 4: The rapidity distributions of  $Z^0$ -bosons in the SM and the LED model, and the corresponding relative discrepancies, defined as  $\delta_{LED}(y^Z) \equiv \left( \frac{d\sigma_{LED}}{dy^Z} - \frac{d\sigma_{SM}}{dy^Z} \right) / \frac{d\sigma_{SM}}{dy^Z}$ , with  $M_S = 3.5, 3.8 \text{ TeV}$  and  $d = 3$ . Figs.4(a), (b) and (c) are for the  $y_T^{Z_1}$ ,  $y_T^{Z_2}$  and  $y_T^{Z_3}$  distributions at the  $\sqrt{s} = 800 \text{ GeV}$  ILC, while (d), (e) and (f) are for the  $y_T^{Z_{1,2,3}}$  distributions at the  $\sqrt{s} = 1 \text{ TeV}$  ILC, respectively.

for specific  $Z^0$ -boson, such as  $Z_1$  (or  $Z_2, Z_3$ ), with different values of  $M_S$  and  $\sqrt{s}$  look to be generally similar. The plots in the Fig.4 show that the curves bulge apparently in the central rapidity region, and the relative discrepancies with  $M_S = 3.5$  (3.8)  $TeV$  can reach about 8% (6%) and 20% (14%) in the central rapidity regions at the  $\sqrt{s} = 800 GeV$  and  $\sqrt{s} = 1 TeV$  ILC, separately. The LED effects intensify the cross section evidently in the central rapidity region of  $|y| < 0.8$  where  $\delta_{LED}(y^{Z_{1,2,3}})$  are all beyond 5%, and the relative discrepancies are basically stable in this region.

In Figs.5(a,b) we present the cross sections in the LED model as functions of  $M_S$  for different  $d$  values at the  $\sqrt{s} = 800 GeV$  and  $\sqrt{s} = 800 GeV$  ILC, separately. The SM cross section which is independent of these two LED parameters is depicted as a horizontal line. Obviously, Fig.5 shows that as the increment of either  $M_S$  or  $d$ , the cross section in the LED model obviously decreases and are getting close to the SM prediction.

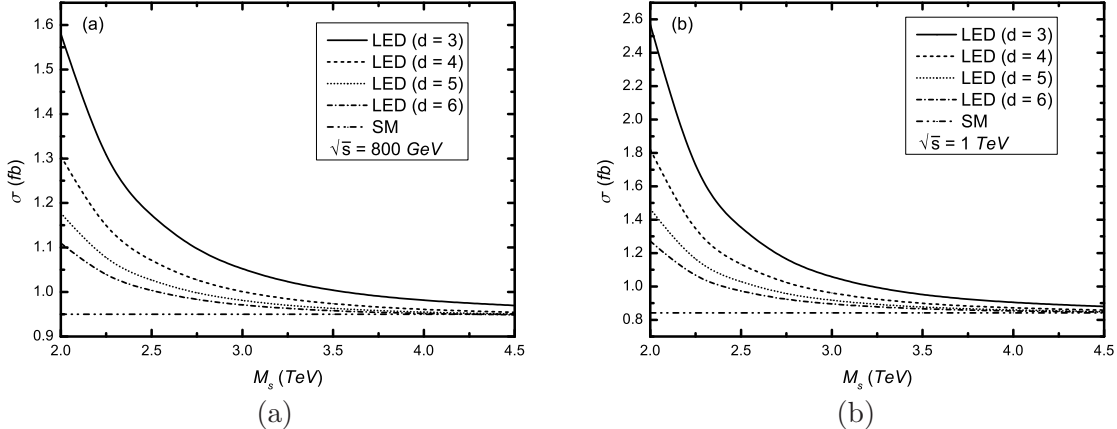


Figure 5: The cross sections in the LED model as functions of  $M_S$  with  $d = 3, 4, 5, 6$ . The additional horizontal line is for the SM cross sections. (a)  $\sqrt{s} = 800 GeV$ . (b)  $\sqrt{s} = 1 TeV$ .

In the following we consider the inclusive process of

$$e^+e^- \rightarrow Z^0 Z^0 Z^0 \rightarrow \mu^+ \mu^- + X, \quad (3.1)$$

where the muons are produced by the subsequential  $Z^0$  decay of  $Z^0 \rightarrow \mu^+ \mu^-$ . We take the branch ratio as  $Br(Z^0 \rightarrow \mu^+ \mu^-) = 3.366\%$  [20]. Since the kinematic distributions of final  $\mu^+$  and  $\mu^-$  are the same, we present the distributions of the transverse momentum of  $\mu$  in both the SM and the LED model,  $\frac{d\sigma_{SM}}{dp_T^\mu}$  and  $\frac{d\sigma_{LED}}{dp_T^\mu}$ , and the corresponding relative discrepancies,

$\delta_{LED}(p_T^\mu)$ , with  $d = 3$ ,  $M_S = 3.5 \text{ TeV}$ ,  $3.8 \text{ TeV}$  and  $\sqrt{s} = 800 \text{ GeV}$ ,  $1 \text{ TeV}$  in Figs.6(a) and (b), respectively. We can read out from the figures that the  $\delta_{LED}(p_T^\mu)$  can reach the maximal values of 10.83% and 7.78% for  $M_S = 3.5 \text{ TeV}$  and  $M_S = 3.8 \text{ TeV}$ , respectively when  $\sqrt{s} = 800 \text{ GeV}$ , while in the case of  $\sqrt{s} = 1 \text{ TeV}$  the maximum values of  $\delta_{LED}(p_T^\mu)$  increase to 29.16% and 20.37% for  $M_S = 3.5 \text{ TeV}$   $M_S = 3.8 \text{ TeV}$ , respectively.

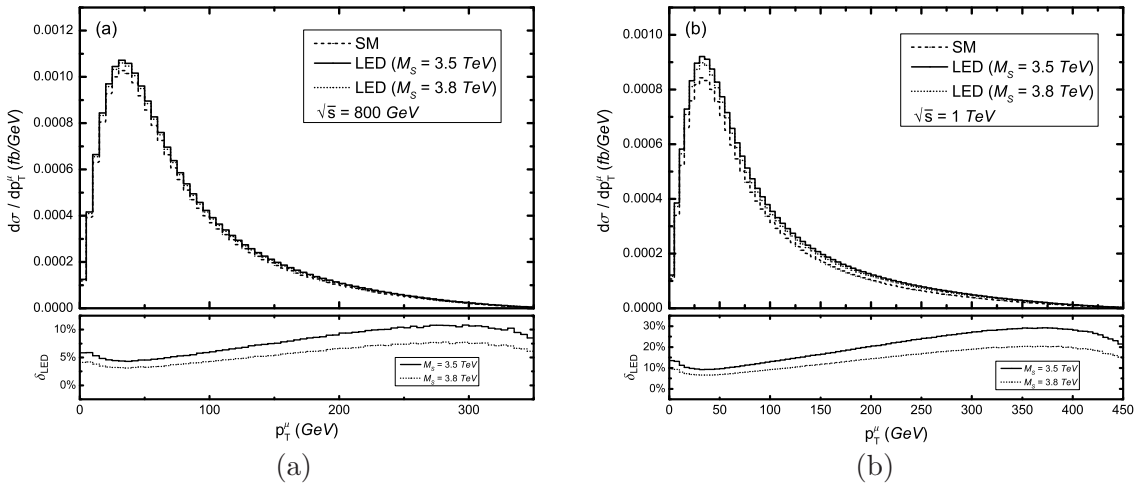


Figure 6: The distributions of the transverse momentum of final muon in the SM and the LED model, and the corresponding relative discrepancies (defined as  $\delta_{LED}(p_T^\mu) \equiv (\frac{d\sigma_{LED}}{dp_T^\mu} - \frac{d\sigma_{SM}}{dp_T^\mu})/\frac{d\sigma_{SM}}{dp_T^\mu}$ ) with  $M_S = 3.5 \text{ TeV}$ ,  $3.8 \text{ TeV}$  and  $d = 3$ . (a) at the  $\sqrt{s} = 800 \text{ GeV}$  ILC. (b) at the  $\sqrt{s} = 1 \text{ TeV}$  ILC.

The rapidity distributions of final muon in the SM and the LED model,  $\frac{d\sigma_{SM}}{dy^\mu}$  and  $\frac{d\sigma_{LED}}{dy^\mu}$ , and the corresponding LED relative discrepancies,  $\delta_{LED}(y^\mu)$ , with  $d = 3$ ,  $M_S = 3.5 \text{ TeV}$ ,  $3.8 \text{ TeV}$  and  $\sqrt{s} = 800 \text{ GeV}$ ,  $1 \text{ TeV}$  are shown in Figs.7(a,b), separately. The curves for the rapidity and the relative discrepancy distributions in the central rapidity regions bulge apparently, and the relative discrepancies have obvious peaks. There  $\delta_{LED}(y^\mu)$  for  $M_S = 3.5 \text{ TeV}$  ( $3.8 \text{ TeV}$ ) can reach 7.5% (5.4%) and 19.1% (13.4%) at the  $\sqrt{s} = 800 \text{ GeV}$  and  $\sqrt{s} = 1 \text{ TeV}$  ILC, respectively.

## IV. Summary

In this paper we study the impact of KK graviton exchange on the scattering process  $e^+e^- \rightarrow Z^0 Z^0 Z^0$  in the LED model at the ILC. This process is very useful in measuring the quartic gauge-boson couplings and probing the existence of extra dimensions. We present the dependence of

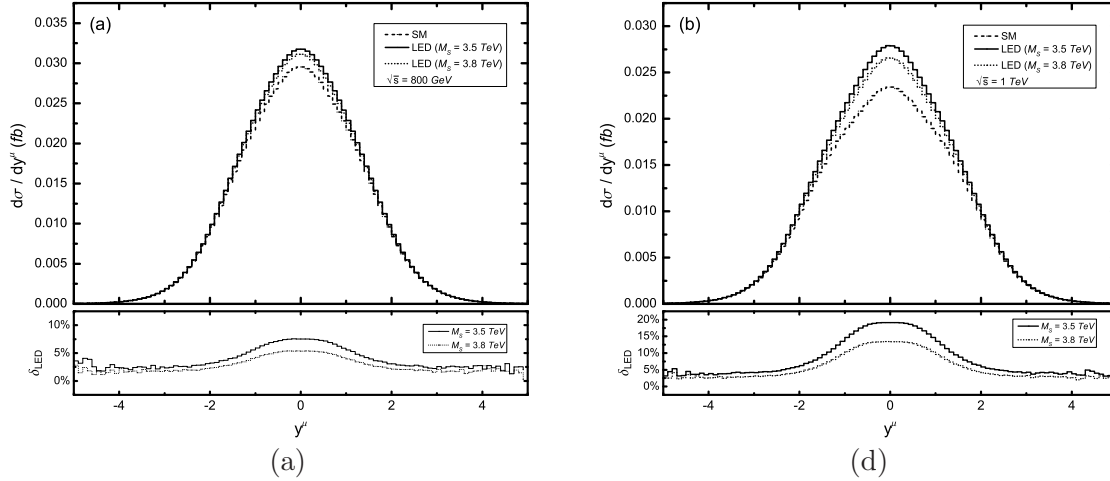


Figure 7: The rapidity distributions of muon in the SM and the LED model, and the corresponding relative discrepancies (defined as  $\delta_{LED}(y^\mu) \equiv (\frac{d\sigma_{LED}}{dy^\mu} - \frac{d\sigma_{SM}}{dy^\mu}) / \frac{d\sigma_{LED}}{dy^\mu}$ ) with  $M_S = 3.5 \text{ TeV}$ ,  $3.8 \text{ TeV}$  and  $d = 3$ . (a) at the  $\sqrt{s} = 800 \text{ GeV}$  ILC. (b) at the  $\sqrt{s} = 1 \text{ TeV}$  ILC.

the cross sections in both the SM and the LED model on the colliding energy  $\sqrt{s}$ , and the kinematic distributions of final  $Z^0$  bosons and their subsequential decay products (muons) at the ILC. We find the contribution from the KK graviton exchange enhances the cross section evidently when  $\sqrt{s}$  goes up beyond  $700 \text{ GeV}$ . We provide also the distributions of the transverse momentum and rapidity of the final produced muon. The results show that the LED effects become more observable in high  $p_T$  ranges or the central region of  $|y| < 0.8$ . We also demonstrate the relationship between the cross sections in the LED model and the fundamental Planck scale  $M_S$  with the extra dimensions  $d$  are 3, 4, 5, 6, respectively.

**Acknowledgments:** This work was supported in part by the National Natural Science Foundation of China (Contract No.11075150, No.11005101, No.11275190), and the Specialized Research Fund for the Doctoral Program of Higher Education (Contract No.20093402110030).

## References

- [1] N. Arkani-Hamed, S. Dimopoulos, and G. Dvali, Phys. Lett. **B429** 263 (1998), arXiv: hep-ph/9803315; Phys. Rev. **D59** 086004 (1999), arXiv: hep-ph/9807344; I. Antoniadis, N. Arkani-Hamed, S. Dimopoulos, and G. Dvali, Phys. Lett. **B436** 257 (1998), arXiv:

- hep-ph/9804398.
- [2] G. F. Giudice, R. Rattazzi, and J. D. Wells, Nucl. Phys. **B544** 3 (1999), arXiv: hep-ph/9811291.
- [3] T. Han, J. D. Lykken, and R. J. Zhang, Phys. Rev. **D59** 105006 (1999), arXiv: hep-ph/9811350.
- [4] K. Agashe, and N. G. Deshpande, Phys. Lett. **B456**, 60 (1999), arXiv: hep-ph/9902263.
- [5] N. Agarwal, V. Ravindran, V. K. Tiwari, and A. Tripathi, Nucl. Phys. **B830**, 248 (2010), arXiv: 0909.2651; Phys. Rev. **D82**, 036001 (2010), arXiv: 1003.5450; M. C. Kumar, P. Mathews, V. Ravindran, and A. Tripathi, Phys. Lett. **B672** 45 (2009), arXiv: 0811.1670.
- [6] S. Ask, Eur. Phys. J. **C60**, 509 (2009), arXiv: 0809.4750. Xiangdong Gao, et al., Phys. Rev. **D81**, 036008 (2010), arXiv: 0912.0199; M. C. Kumar, P. Mathews, V. Ravindran, and S. Seth, Nucl. Phys. **B847**, 54 (2011), arXiv: 1011.6199.
- [7] V. Hankele, and D. Zeppenfeld, Phys. Lett. **B661**, 103 (2008), arXiv: 0712.3544; J. Bagger, V. Barger, K. Cheung, J. Gunion, T. Han, G.A. Ladinsky, R. Rosenfeld, and C.-P. Yuan, Phys. Rev. **D49** 1246 (1994), arXiv: hep-ph/9306256; **D52** 3878 (1995), arXiv: hep-ph/9504426.
- [8] A. Lazopoulos, K. Melnikov, and F. Petriello, Phys. Rev. **D76**, 014001 (2007), arXiv: hep-ph/0703273.; G. Bozzi, et al., Phys. Rev. **D81**, 094030 (2010), arXiv: 0911.0438.
- [9] T. Binoth, G. Ossola, C.G. Papadopoulos, and R. Pittau, JHEP **0806**, 082 (2008), arXiv: hep-ph/0804.0350.
- [10] Su Ji-Juan, Ma Wen-Gan, Zhang Ren-You, Wang Shao-Ming, and Guo Lei, Phys. Rev. **D78**, 016007 (2008), arXiv: 0807.0669.
- [11] F. Boudjema, Le Duc Ninh, Sun Hao, and M. M. Weber, Phys. Rev. **D81**, 073007 (2010), arXiv: 0912.4234.

- [12] M. C. Kumar, P. Mathews, V. Ravindran, and S. Seth, Phys. Rev. **D85**, 094507 (2012), arXiv: 1111.7063.
- [13] A. Djouadi, J. Lykken, K. Mönig, Y. Okada, M. Oreglia, S. Yamashita, et al., arXiv:0709.1893, ILC Reference Design Report, <http://www.linearcollider.org/about/Publications/Reference-Design-Report>.
- [14] Bai Yu-Ming, Guo Lei, Li Xiao-Zhou, Ma Wen-Gan, and Zhang Ren-You, Phys. Rev. **D85**, 016008 (2012), arXiv: 1112.4894.
- [15] Zhou Ya-Jing, and Xing Li-Rong, Phys. Rev. **D78**, 055021 (2008).
- [16] T. Hahn, Comput. Phys. Commun. **140**, 418 (2001), arXiv: hep-ph/0012260.
- [17] T. Hahn, and M. Perez-Victoria, Comput. Phys. Commun. **118**, 153 (1999), arXiv: hep-ph/9807565.
- [18] ATLAS Collaboration, 'ATLAS experiment presents latest Higgs search status', [<http://www.atlas.ch/news/2011/status-report-dec-2011.html>]; CMS Collaboration, "CMS search for the Standard Model Higgs Boson in LHC data from 2010 and 2011", [<http://cms.web.cern.ch/news/cms-search-standard-model-higgs-boson-lhc-data-2010-and-2011>].
- [19] Web site: <http://comphep.sinp.msu.ru/>.
- [20] J. Beringer et al. (Particle Data Group), J. Phys. **D86**, 010001 (2012).
- [21] ATLAS Collaboration, 'ATLAS experiment presents latest Higgs search status', [<http://www.atlas.ch/news/2011/status-report-dec-2011.html>]; CMS Collaboration, 'CMS search for the Standard Model Higgs Boson in LHC data from 2010 and 2011', [<http://cms.web.cern.ch/news/cms-search-standard-model-higgs-boson-lhc-data-2010-and-2011>].
- [22] ATLAS Collaboration, arXiv: 1112.2194.
- [23] CMS Collaboration, arXiv: 1112.0688; arXiv: 1202.3827.